JOURNAL OF SPACECRAFT AND ROCKETS
Vol. 33, No. 4, July–August 1996

Large-Angle Articulated Beam Truss Design Methodology Considering Offset Joint Modeling

Gregory Thorwald* and Martin M. Mikulas Jr.†
University of Colorado, Boulder, Colorado 80309

Adaptive space structures (deployable trusses, large space antennas) can use actuated members to vary their geometry. In particular, variable geometry trusses can use the same set of actuators for both deployment and subsequent articulation. Such articulating trusses can be applied in space crane orbital construction applications. Previous structural analyses have used idealized truss models; members connect at a point at each node. Further analysis of practical truss models in articulated geometries will show the difference in structural behavior compared to ideal trusses and the need to include realistic geometric modeling, such as including the hinge offsets to give the correct packaged truss geometry. An analytic example truss verifies the finite element modeling technique used. Stiffness sensitivity trends for a range of articulated geometries reveal two causes of stiffness reduction: decreased truss effective bending inertia because of shortened actuators and batten bending caused by asymmetric geometry and hinge offsets. The analyses lead to a structural design methodology, including an initially curved geometry, to alleviate the stiffness reduction for improved structural performance. The initially curved articulating truss allows the location of maximum stiffness to be designed and provides compact packaging, self-deployment, and geometric articulation.

Nomenclature

A	= area of member cross section, in.^{2}
c	= diagonal member length, in.
d_i	= batten actuation distance, in.
E	= Young's modulus of elasticity, psi
F	= axial bar force, lb
f	= vibration frequency, Hz
h	= height of truss, batten member length, in.
I	= area moment of inertia, in.^{4}
J	= Jacobian gradient matrix, in.
K	= structural stiffness, lb/in.
L	= total truss length, in.
l	= longeron member length, in.
l_1, l_2, l_3	= hinge-offset lengths, in.
M	= mass, lb-s^2/in., bending moment, in.-lb
n_x, n_y	= x and y components of l_2 hinge offset, in.
P	= applied load, lb
p_1, p_2	= batten actuator length multiplier, scalar
R	= curved truss radius of curvature, in.
U	= strain energy, in.-lb
W	= weight, lb
x, y	= node coordinates, in.
$\alpha, \beta, \phi, \omega$	= ideal-truss kinematics angles, deg
γ_n	= curved truss increment angle, deg
Δ	= analytic displacement, in.
θ	= total arc angle, batten member orientation angle, deg
μ, ξ	= substitution parameters
ρ	= density, lb-s^2/in.^{4}
Ψ	= truss articulation secant angle, deg

Introduction

ADAPTIVE structures can beneficially alter their characteristics, geometry in particular, in a controlled manner. Deployable structures, space cranes, large space antennas, and variable geometry truss booms utilize hinged and prismatic actuated members to vary their geometry. Deployable structures can be compactly packaged for transportation and then deployed to full size for use. If a space structure is too large for a single launch, such as a space station or interplanetary spacecraft, space cranes or adaptive truss manipulators can aid in orbital construction. In a terrestrial application, articulating truss arms could be used in hazardous waste clean up, such as in a nuclear reactor. These applications are possible by capitalizing on the desirable features of articulating trusses: compact packaging, a repeating structural pattern, actuation for variable geometry and self-deployment, and a kinematic redundancy from many available actuators.

Space cranes[1] resemble conventional robots with trusses replacing the arm links and length extending actuators replacing the rotational joints. Wu and Sutter[2] analyzed three space crane articulated joint concepts. Dorsey et al.[3] stated that desirable features of space cranes include structural adaptability, structural predictability (implying correct structural modeling is important), and precision manipulation of massive payloads.

Variable geometry trusses (VGTs) present the possibility of self-deployable structures able to use the deployment actuators to alter each bay's geometry, giving serpentine cranelike articulation. VGTs are attractive for use in construction roles since they provide a stable structure even in partially deployed or articulated geometries. Several specific VGT concepts using a stacked regular octahedral geometry have been examined. Rhodes and Mikulas[4] and Mikulas et al.[5] developed and patented the concept of a stacked-octahedral controllable-geometry truss beam that does not require a deployment mechanism. The six diagonal members have a fixed length and the three lateral battens have a variable length in alternate bays, compared to a Stewart[6] platform where the six diagonals change length and the three lateral members have a fixed length. Subsequently, Miura and Furuya[7] proposed using the lateral members in every batten plane for actuation. Miura and Furuya[8] added structural error analysis and deployment vibration analysis. Hughes et al.[9] found the stacked octahedral geometry to excel in its structural properties. Chen and Wada[10] also used the stacked octahedral geometry for an adaptive truss manipulator (ATM); ATM benefits include compact stowage, high dexterity, and actuator redundancy.

Kinematic and inverse kinematic solutions of articulating trusses provide understanding of the articulating motion through determination of the truss geometry given the actuator lengths.[11] In Ref. 12 the inverse kinematics of a truss space crane including the induced flexible motion were solved. Padmanabhan et al.[13] derived the inverse kinematics of a double and quadruple octahedral VGT. Tanaka et al.[14] studied the kinematics of a more practical truss model; the hinges are offset away from the truss node as a practical design consideration to avoid a more complex joint connecting multiple

Received July 20, 1994; revision received June 27, 1995; accepted for publication Aug. 25, 1995.

*Graduate Student, Aerospace Engineering Department.
†Professor, Aerospace Engineering Department. Member AIAA.

members at a single node. Comparing the resulting geometry of ideal and practical truss models reveals that the ideal model is too simple to realize the kinematics of the practical model. Given the same set of actuator lengths, the two truss models will have a different final geometry.

Objectives

All of the structural analysis in the references have used idealized truss models: all members connect at a point at the truss node. Further study of practical truss models (hinge offsets are included) will show the difference in structural behavior compared to ideal-truss models and the need to include practical modeling considerations in deployable-articulated trusses. The deployable-articulated truss structure design methodology presented herein continues the analysis presented by Mikulas et al.[15] In the deployment analysis, hinge offsets were included to account for the finite member sizes when packaged. In a slewed or articulated configuration, asymmetric geometry relative to a batten occurs. It was hypothesized that the resulting bending moments acting on the batten actuator element could cause the overall truss stiffness to be reduced, and this was confirmed in Ref. 16.

The structural behavior of ideal and offset trusses in articulated configurations are compared by quantifying the difference from computed structural stiffness sensitivity trends. Strategies are then developed to alleviate the observed stiffness reduction and improve the structural performance. A structural design methodology for articulating trusses is developed from these strategies. The design methodology includes an alternative initially geometry. The initially curved articulating truss (ICAT) is designed to begin within the operational region rather than having to first actuate to a functional position. The ICAT packages compactly and can self-deploy.

By using kinematic solutions of the truss example for a range of articulated geometries with finite element eigenvalue analysis, stiffness sensitivity trends for the given truss models are computed. Analytic stiffness results are compared to finite element computed values to verify the modeling technique used in examining the effect of hinge offsets.

Structural stiffness reduction in articulated configurations is caused by two mechanisms. First, as the batten actuators shorten to increase the amount of articulation, the effective bending inertia (EI) of the truss decreases due to a notching effect in the truss geometry that reduces the overall stiffness (affects both ideal and offset truss models). Second, in an actuated geometry, bending moments are applied to the battens by the asymmetric member geometry or by asymmetric loads from neighboring truss members; see Figs. 1 and 2. The resulting batten bending in the offset-truss model causes additional stiffness reduction indicating the need to include the hinge offsets in VGT models.

Distributing the actuation of the truss by using several actuators and using extending actuators for articulation diminishes the notching effect. Strategies to reduce batten bending in the offset-truss model include increasing the batten moment of inertia of the members (bending stiffness) and modifying the hinge-offset lengths. These approaches modify an existing truss. By giving the articulated truss an initially curved geometry, the maximum structural stiffness

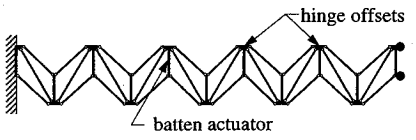

Partially deployed truss

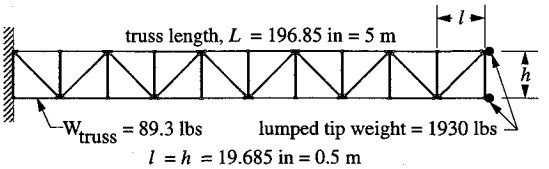

Deployed truss

Fig. 1 Deploying truss.

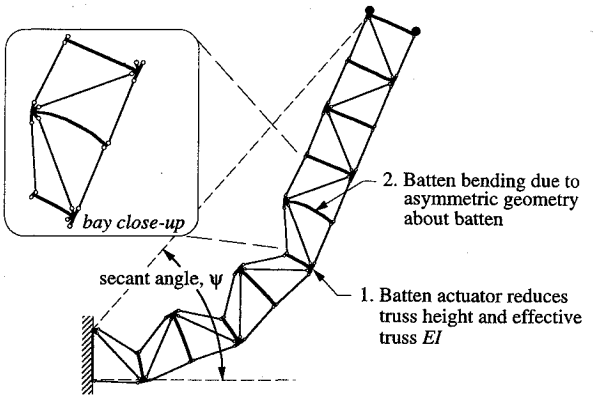

Fig. 2 Articulating truss.

is shifted to the desired position. The given position of the ICAT can be chosen so that the maximum structural stiffness is obtained in the primary operational region of the articulated truss.

Truss Model Types and Kinematic Analysis

A long repeating geometry truss used as an articulating arm is beamlike in its behavior. When moving a payload, the truss behaves similar to a beam with a lumped mass at the free end. The vibration frequency for a cantilever beam with tip mass is given as[17]

$$f_{\text{beam}} = \frac{1}{2\pi}\sqrt{\frac{3EI}{L^3(M_{\text{tip}} + 0.24M_{\text{beam}})}} \tag{1}$$

To apply this equation to the corresponding uniform truss, the moment of inertia is replaced by the effective inertia of the truss. Sketch A shows the cross section of the planar, two-longeron truss:

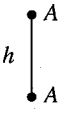

$$I = 2\left(\frac{h}{2}\right)^2 A = \frac{Ah^2}{2} \tag{2}$$

Substitution of Eq. (2) into Eq. (1) gives the vibration frequency for a uniform truss.

For a beam or a truss, the terms that can be modified to increase the frequency are geometric: I, A, and h; or material: E and mass (modify the density). The improvement available in the modulus or density is limited by available materials, leaving geometric improvements. An increase of the cross-sectional area or height of the truss members, corresponding to increasing the moment of inertia, will give a frequency increase until the additional mass becomes detrimental enough to curtail further improvement. Modifying these geometric parameters provides a starting point and indicates that additional geometric modifications will improve the performance of the articulated truss. A finite element model of the truss will allow the effect of articulating geometry to also be determined for both truss model types as that behavior is not accounted for in the previous equations.

Ideal-truss models are often chosen for structural analysis because the structural behavior can be determined analytically and is the easiest to model and analyze in a finite element routine. Such a model is appropriate in the case of a structure whose geometry is fixed and for preliminary analysis of more complex structures. The endpoints of the truss members connect at the mathematical intersection point (as modeled for finite element analysis). Here, the ideal truss will be used for comparison to the more realistic offset-truss model. Figure 3 shows a single bay of an ideal truss.

The realistic offset-truss model includes the geometric offset lengths to the hinge locations from the vertex node point (Fig. 4). The offsets are necessary for deployable type trusses to account for the finite size of the truss members in the packaged configuration. The offset truss is designed so that when fully deployed the member centerlines will intersect at the mathematical node point. In the fully deployed geometry, the offset truss does behave as a true truss.

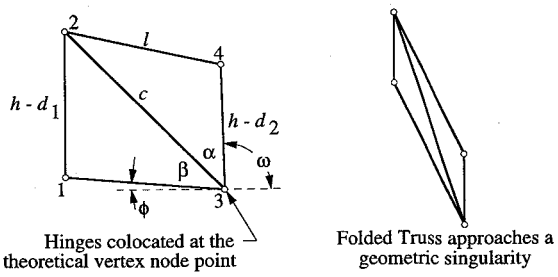

Fig. 3 Articulating ideal-truss kinematics: strut radius not considered; d_i is the amount each batten actuator has been shortened.

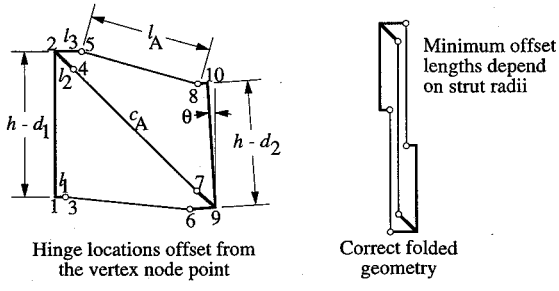

Fig. 4 Articulating offset-truss kinematics: accounts for finite radius of struts; same number of hinges and actuators as ideal truss; modeling requires more nodes, more elements; l, h = bay dimensions, l_A = longeron length, c_A = diagonal length, and l_1, l_2, l_3 = offset lengths.

An ideal truss has a geometric singularity when packaged because the members and node points become coincident (an unrealistic geometry). The offset truss also reaches a singularity when packaged because of the members being parallel to one another. The singularity is structural in nature because mathematically the structure could deploy in either direction. The offset singularity can be overcome by providing a bias in the direction of deployment by not completely packaging the truss (the truss is left slightly in the direction of deployment) or by using preload springs pushing in the preferred deployment direction.

The selection of the actuator location is based on the total number of actuators required in a truss, the anticipated member loads in the actuator, as well as using the actuator for both deployment and subsequent articulated motion. As determined in Ref. 15, replacement of the batten members by actuators best meets the requirements. The batten location gives nearly the lowest total number of actuators, and are also not in the direct load path. The batten location also allows the truss to be actuated to any desired geometry.

The kinematic solutions of the articulated truss models are needed as a preprocessing step in the analysis sequence. Given the actuator lengths, the node coordinates are determined from the kinematic solution. To develop a sensitivity trend of a structural parameter, the actuator lengths are incremented through a range of values; the node coordinates are updated for each geometry and used in the input data for eigenvalue analysis.

The ideal-truss kinematics can be directly determined because the geometry remains triangular for all actuator lengths. Figure 3 shows the angles and lengths used to determine the node coordinates. The offset-truss kinematics become a set of coupled constraint equations for each truss bay due to the offset lengths. In a general configuration, the offset truss no longer has the simple triangular geometry. Refer to Fig. 4 for the parameters used to determine the node coordinates. The iterative solution finds the position and orientation of the next batten member that satisfies the length constraints of the three connecting members (two longerons and a diagonal), while keeping the offset lengths fixed relative to each batten. Refer to the Appendix for the kinematic solutions.

Structural Sensitivity Trend Studies

The stiffness of a structure gives an indication of the structural performance capability. For a structure whose behavior is dominated by a single mode, the square of the first natural vibration frequency gives a direct measure of the stiffness (structural mass is constant). Such a structure is examined here: a planar beam-like truss with a large tip mass,

$$f^2 \approx K/M \approx \text{structural stiffness} \tag{3}$$

A general function can indicate the dependence of the truss stiffness on several parameter values:

$$f^2 = F(\text{number of actuators, method of actuation, secant angle, batten inertia, offset lengths, member areas, truss height}) \tag{4}$$

Modifying each parameter in turn reveals its effect on the stiffness. Finite element analysis is used to calculate the resulting stiffness (frequency squared) trends for changes in each parameter through a range of articulation. Although the ratio of static applied load to corresponding displacement would also give the stiffness, the required applied loading of a more complex structure that results in the same deformed shape as the lowest frequency mode may not be known. For complex structures eigenvalue or frequency analysis is preferable to static load analysis because the eigenvector reveals the lowest stiffness shape of the structure.

The values for the geometry and materials used in the example are representative of an experimental 2-bay batten actuated truss currently being developed.[18] Refer to Fig. 1 for a diagram of the 10-bay example truss. For both the ideal- and offset-truss models, every batten is an actuator, 11 in total. The offset truss has the offset lengths (designed for the experimental truss) incorporated between the battens and hinges. The short, medium, and long offset length l_1, l_2, and l_3 are 0.50, 1.503, and 1.625 in., respectively. The strut properties (longerons and diagonals) are for aluminum tubing and the batten properties are for solid stainless-steel lead-screws (a solid slender cylinder that has a continuous thread along its length). For the ideal-truss model members (longerons and diagonals), the material values are $E = 10 \times 10^6$ psi, $\rho = 0.0031$ lb-s^2/in.^{4}, and $A = 0.0673$ in.^{2} The offset-truss model uses the same values for the members but with an area of $A = 0.0633$ in.^{2} so that the deployed trusses have equivalent stiffness. The batten members in both truss models have values of $E = 28 \times 10^6$ psi, $\rho = 0.0089$ lb-s^2/in.^{4}, $A = 0.0511$ in.^{2}, and $I = 2.0755 \times 10^{-4}$ in.^{4}. The hinge-offset members use the same values as the batten members with a 100 times larger moment of inertia $I = 2.0755 \times 10^{-2}$ in.^{4} since the offset members are solid machined parts having a much higher moment of inertia than other members. The total structural mass is 0.231 lb-s^2/in. (weight = 89.3 lb), and the large tip mass (half at the top and bottom of the last batten) is 5.0 lb-s^2/in. (tip weight = 1930 lb). The tip mass, more than 20 times the structure's mass, is added to represent a payload being manipulated by the articulating truss. The large tip mass drives the truss frequency lower making beamlike bending the dominant behavior.

For the finite element analysis, the longerons and diagonals are modeled by bar elements, and the battens are modeled by five beam elements per member for both truss types. The offset elements are modeled by single beam elements (rotational degrees of freedom are connected between offsets and battens).

Since the articulated truss geometry for given actuator lengths is different for the ideal- and offset-truss models, a common geometric parameter is required. Figure 2 also shows how the secant angle is measured from the top node of the first batten to the top node of the last batten with respect to the horizontal. When the truss is straight, the secant angle is zero.

Using the given material values and dimensions, stiffness values are computed for a range of actuator lengths for both the ideal and offset trusses. Figure 6 shows several stiffness trends for the offset- and ideal-truss models. A nondimensional stiffness (frequency squared multiplied by the appropriate parameters) is used for generality. Figure 5 shows corresponding articulated truss geometries. The trends demonstrate the difference of behavior of ideal and offset models. The stiffness decreases for both trusses with increasing articulation, but more rapidly for the offset truss, especially when just one actuator is used to provide the articulation. At zero secant angle, both truss models have the same stiffness. Five actuators distribute the articulation along the truss that increases the

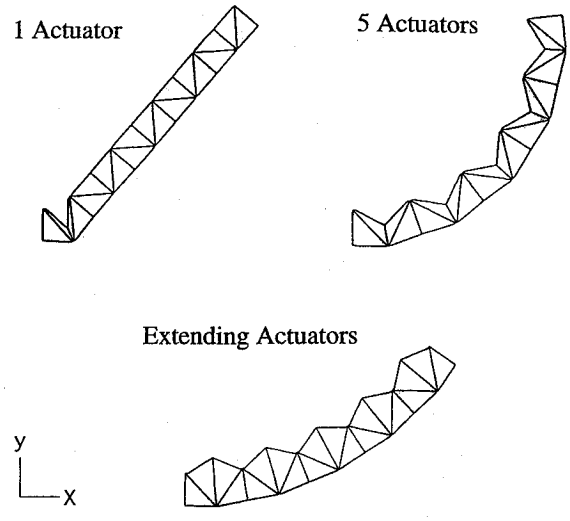

Fig. 5 Examples of articulating trusses.

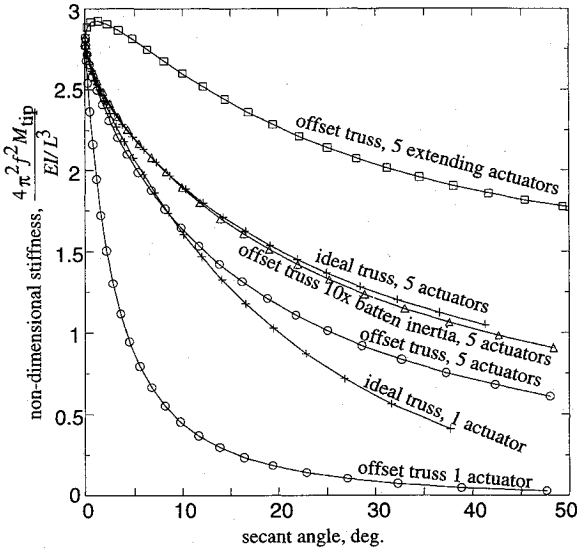

Fig. 6 Stiffness trends during articulation.

overall stiffness for both models. Compared to using a single actuator, the offset truss using five actuators has a stiffness increase of 6.8 times at 20-deg secant angle and an increase of 18.7 times at 40 deg. Increasing the moment of inertia of the battens verifies that batten bending causes additional stiffness reduction in the offset truss (no batten bending in the ideal model). With stiffer battens, the offset truss stiffness is improved to near the ideal trend (using five actuators). The stiffer battens improve the offset stiffness 1.3 times at 20 deg compared to the five-actuator offset truss, and increases the stiffness 1.4 times at 40 deg. If additional batten length is available for articulation, the actuators can be extended, again improving the stiffness while articulated.

Other modifications that can be made to the truss to improve structural stiffness include modifying the hinge-offset lengths to their minimum length, increasing the truss height, redistributing the truss mass by modifying the member cross-sectional areas. These methods did not give as significant an increase as the previously mentioned methods, and their results are not plotted.

Analytic Truss Example

A one-and-a-half-bay truss is used as the analytic example for comparison to finite element computed stiffness results to verify the modeling technique used. The structure has been simplified to just a single offset located on the top longeron. For the analytic truss example, the top offset is the most important in affecting the overall stiffness because it is the only member able to apply a bending moment to the batten (only the top longeron will change orientation).

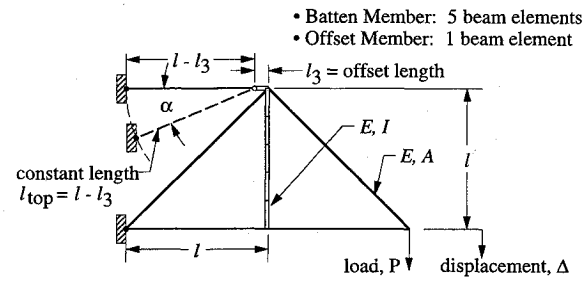

Fig. 7 Sketch of analytic and finite element truss model.

A transverse vertical load P is applied to the right end of the truss. To represent batten actuator shortening on the left side of the truss (at the boundary supports), the top longeron is rotated downward through the angle α from its initial horizontal position, $\alpha = 0$ (Fig. 7).

To use Castigliano's theorem[19] to obtain the analytic deflection of the truss, the member loads must first be determined from static force equilibrium. Then, all of the member strain energies are summed. Taking the derivative of the total strain energy with respect to the applied load, the analytic displacement is obtained. The strain energy in individual bar and beam members for use in Castigliano's theorem is given as

$$U_{bar} = \frac{F^2 L}{2EA} \qquad U_{beam} = \frac{1}{2EI}\int_0^L M^2(x)\,dx \tag{5}$$

After differentiation with respect to the force P, the displacement is

$$\Delta = \frac{\partial U}{\partial P} = P\left\{\frac{(2\sqrt{2}+1)l}{EA} + \left[\frac{l\cos\alpha(1+\xi)}{\mu} - \xi - 1\right]^2 \times \frac{l^3}{3EI} + \left[\frac{l(1+\xi)}{\mu}\right]^2 \frac{(l-l_3)}{EA} + \frac{2\sqrt{2}l\xi^2}{EA} + \left[\frac{l\cos\alpha(1+\xi)}{\mu} - \xi\right]^2 \frac{l}{EA} + \left[\frac{l\cos\alpha(1+\xi)}{\mu}\right]^2 \frac{l_3}{EA} + \left[\frac{l\sin\alpha(1+\xi)}{\mu}\right]^2 \frac{l_3^3}{3EI}\right\} \tag{6}$$

where the substitution parameters (for simplification) are defined as follows:

$$\mu = l_3\sin\alpha + l\cos\alpha \qquad \xi = \frac{1 + l\sin\alpha/\mu}{1 - l\sin\alpha/\mu} \tag{7}$$

The truss stiffness is given by the P/Δ ratio using the displacement from Eq. (6):

$$\Delta/P = 1/K \quad \text{or} \quad P/\Delta = K \tag{8}$$

A set of stiffness sensitivity trends are computed for the analytic stiffness K. Each trend depends on the rotation of the top longeron (batten shortening) and on the offset length. The stiffness trend plots use the following values for the structural parameters (based on the 10-bay example truss in Fig. 1): $E = 10 \times 10^6$ psi, $\rho = 2.59 \times 10^{-4}$lb-s^2/in.^{4}, $A = 1.0$ in.^{2}, $I = 7.96e\text{-}2$ in.^{4}, $P = 10$ lb, $l = 20$ in., and the offset length l_3 is from 0 to 10% of l.

Figure 8 shows that as the top longeron is rotated the overall truss stiffness decreases, just as for a shortened actuator. As expected, the stiffness decrease is more pronounced as the offset length is increased to 5 and 10% of the longeron length. The data points on the plot show the computed truss stiffness values (the lines give the analytical stiffness values). The analytic stiffness trend matches to within 0.1% of the finite element computed values indicating that the finite element model sufficiently models the behavior.

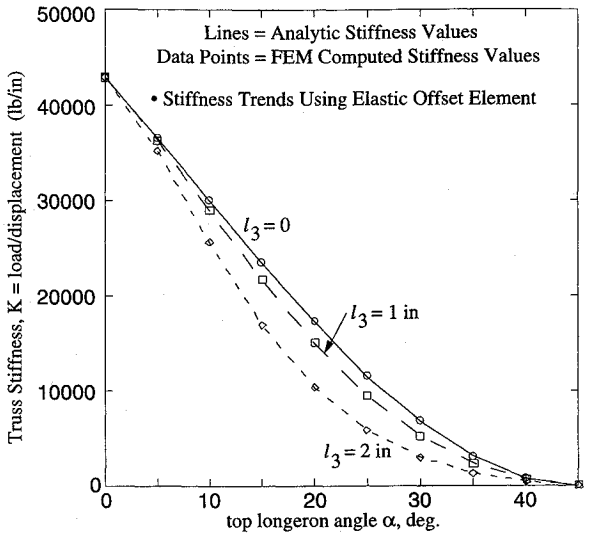

Fig. 8 Analytic and finite element stiffness results.

Initially Curved Deployable-Articulated Truss

An adaptive truss used as an articulated arm will generally have a curved operational configuration. That is, the truss will not often operate at its straight, fully deployed geometry; instead, it will operate at some position within its operational region that will require it to be in an actuated configuration. An articulating truss is a true or perfect truss structure (member centerlines pass through a single point at each node) in only one position; with any articulation, the truss deviates from that perfect geometry. The deployed geometry giving the true truss structure can be chosen. To improve the structural stiffness of the truss, the initial geometry is designed to be curved (based on a circular arc). As the ICAT operates, the geometric configuration is perturbed about the initially curved position.

Figure 9 shows the relation between the secant angle, the total arc angle, radius of curvature, and the truss length that are used to determine the node coordinates:

$$\theta = 2\psi \qquad R = L/\theta \tag{9}$$

The ICAT is designed with both the top and bottom longerons perpendicular to the middle batten members to avoid double-valued kinematics and to keep a larger truss height. Figure 10 shows the two-bay repeating truss cell with hinge offsets included.

The bottom longeron, top longeron, and middle batten lengths are given by

$$l = R\sin\theta_b, \qquad l_{\text{top}} = (R+h)\sin\theta_b, \qquad h_2 = h\cos\theta_b \tag{10}$$

These equations indicate that with four parameters—the total arc length of the truss, the design secant angle, the batten length, and the number of bays—the other parameters are determined.

The ICAT packages compactly but now has two different actuator lengths to account for the different top and bottom longeron lengths given approximately by

$$p_1 h \cong c + \sqrt{2}l_2 - l \qquad \text{and} \qquad p_2 h_2 \cong c + \sqrt{2}l_2 - l_{\text{top}} \tag{11}$$

where the $\sqrt{2}l_2$ term approximately represents the horizontal component of the diagonal offset.

For the initially curved truss, the coordinate for the center of curvature is given by the arc radius, and the increment angle is increased for each bay along the curved truss:

$$(x_0, y_0) = (R, 0), \qquad \gamma_n = (n-1)\theta_b \qquad n = 1, 2, 3, \ldots, n_{\text{bay}} + 1 \tag{12}$$

When the bay number n is odd, the node coordinates are given by

$$\begin{aligned} x_{\text{bottom},n} &= x_0 - R\cos\gamma_n & x_{\text{top},n} &= x_0 - (R+h)\cos\gamma_n \\ y_{\text{bottom},n} &= y_0 + R\sin\gamma_n & y_{\text{top},n} &= y_0 + (R+h)\sin\gamma_n \end{aligned} \tag{13}$$

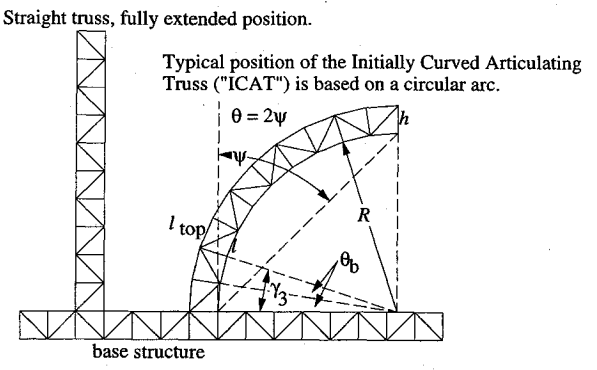

Fig. 9 Comparison of initially curved and straight trusses.

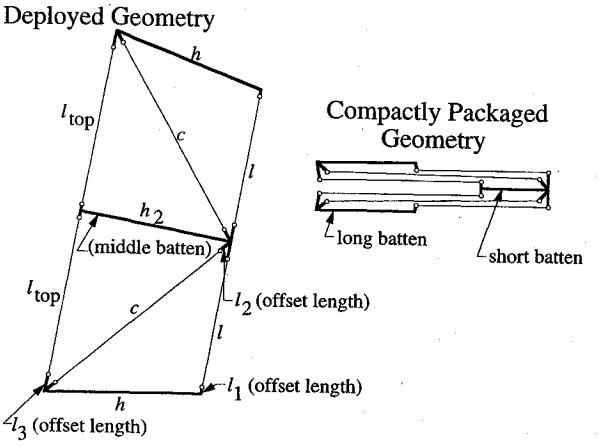

Fig. 10 Repeating two-bay cell for curved truss.

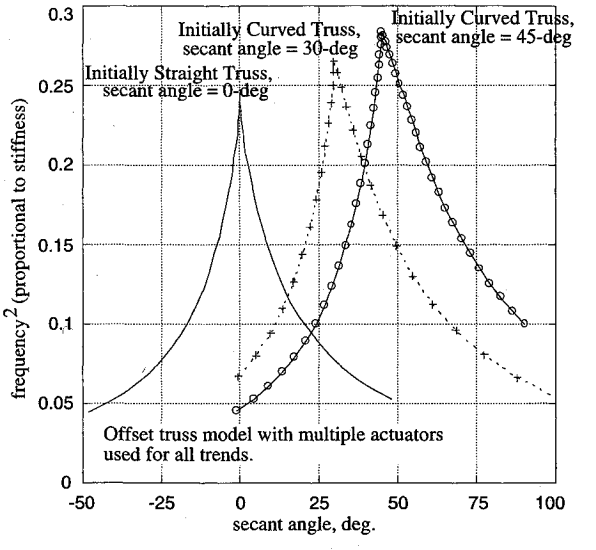

Fig. 11 Maximum stiffness location.

and when n is even (middle battens),

$$\begin{aligned} x_{\text{bottom},n} &= x_0 - (R\cos\theta_b)\cos\gamma_n \\ x_{\text{top},n} &= x_0 - [(R+h_2)\cos\theta_b]\cos\gamma_n \\ y_{\text{bottom},n} &= y_0 + (R\cos\theta_b)\sin\gamma_n \\ y_{\text{top},n} &= y_0 + [(R+h_2)\cos\theta_b]\sin\gamma_n \end{aligned} \tag{14}$$

Using these equations, the basic geometry (vertex node points) of the ICAT is computed; additional node points for the hinge offsets are added using the vertex nodes as a basis.

Stiffness trends for two initially curved trusses designed at 30- and 45-deg secant angle are computed and compared to an initially straight truss (0-deg secant angle) (Fig. 11). For the analysis, all of

the trusses are articulated upward and downward from their initial design position through a total of 90-deg sceant angle. Figure 11 shows that the peak stiffness can be shifted from one initial position (secant angle) to another by using the initially curved truss design. For example, if the primary operational region of the articulated truss is at a given angle, the truss is designed to have its peak stiffness value at that position. Then as the articulated truss operates about that primary position, the overall truss stiffness is perturbed from the peak value. The previous improvements (increased batten stiffness) can also be applied to the ICAT.

Analysis of Three-Dimensional Truss Model

Having determined that the design strategies and initially curved geometry improve the structural stiffness for the planar trusses, the analysis continues for a three-dimensional truss example (Fig. 12). While the planar truss models demonstrated the truss improvements, it is necessary to analyze a full three-dimensional truss model to determine whether other behavior affects the truss performance, such as a low-frequency torsional mode not present in a planar model. If no unexpected behavior occurs, a less complex planar truss model may be used in place of the more complex three-dimensional truss for analysis.

The three-dimensional offset-truss model is based on the planar offset-truss model. The front and back faces of the three-dimensional truss follow the same lacing pattern or topology as the planar example. There are no diagonals in the batten planes, rather the internal diagonals attach to opposite corners through the interior of the bay, top back left corner to bottom front right corner, for example. No diagonals may be present in the batten plane as the height of that cross section varies as the truss is actuated. There are two batten actuators per bay (front and back faces of the truss). The top and bottom truss planes as well as the diagonal planes (which includes the internal diagonal) remain fixed in their geometry as the truss articulates in a plane. For out-of-plane articulation, a rotary joint at the base of the truss would provide rotation of the truss. Another set of batten actuators on the top and bottom of the truss could also provide transverse articulation.

For the analysis, the truss is again 10 bays in length and the same amount of lumped mass previously used is distributed at the four nodes at the end of the truss. To simulate a module-sized payload, the lumped mass is extended to each side from the end of the truss by a massless structure using rigid elements. The rotational mass moment of inertia for the payload is now 13 times greater than without using the simulated five-bay-wide module.

For the three-dimensional offset truss, the stiffness trends for the first three modes for the initially straight and curved truss are shown in Fig. 13. The first mode combines transverse bending in the z direction at the end of the truss with torsional motion near the base to give a dominant transverse bending motion. The torsion increases as the design secant angle is increased, which causes the peak stiffness of mode 1 to decrease with increasing design curvature. Mode 2 has bending motion is in the vertical, y direction. Mode 3 has some

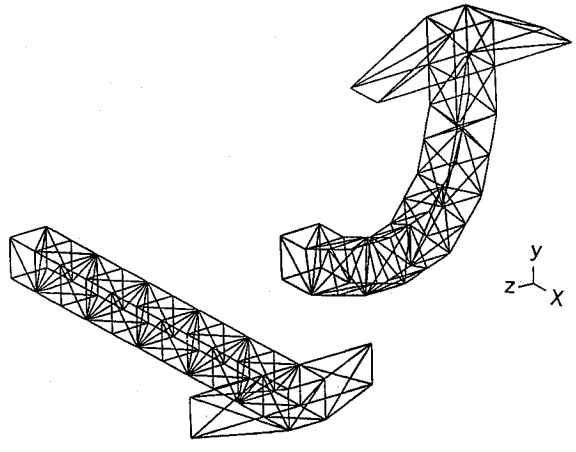

Fig. 12 Initially straight and curved three-dimensional trusses with simulated payload module.

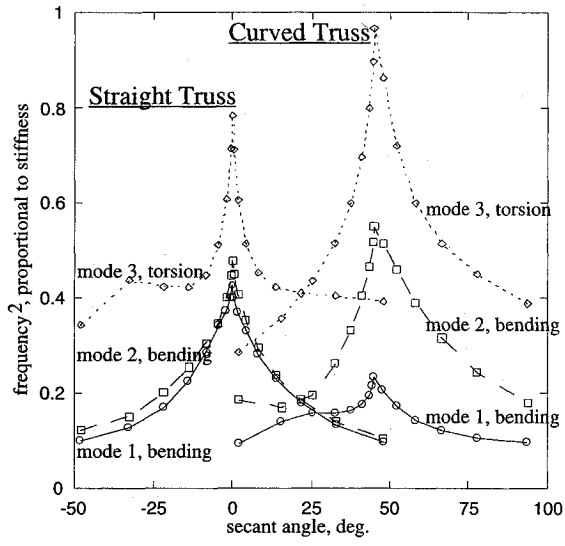

Fig. 13 Maximum stiffness shift for each mode.

bending near the base but is dominated by torsion of the payload about the truss. As Fig. 13 shows, the torsional mode remains above both bending modes throughout the articulation even with the module present. Without the payload module, the torsional mode has a corresponding 13 times higher frequency. Although the peak stiffness of mode 1 decreases in the ICAT design, that stiffness remains above the initially straight truss stiffness after articulating to the same position. If the primary region of operation is known, the three-dimensional ICAT gives better truss performance than having to first articulate from another geometry. The planar truss model continues to be valuable for preliminary analysis including packaging, deployment, and articulation strategies. The initially curved geometry is also applied to the three-dimensional truss. Again, the peak stiffness is shifted to the design secant angle. Figure 13 shows that the peak stiffness value for all three modes (bending and torsional) is shifted.

Conclusions

A structural design methodology was developed to improve structural performance in deployable-articulated trusses that include hinge offsets to account for finite size members. The structural stiffness was quantified by computing stiffness sensitivity trends for a range of articulated geometries. Whereas structural stiffness was observed to decrease for both ideal and offset-truss models in articulated configurations, the decrease was greater for the offset truss, indicating the need to include the hinge offsets (the length from the hinge connection with longeron and diagonal members to the theoretical node point). Batten actuators provide the capability for the truss to articulate through large angles and also to self-deploy. Such articulated or variable geometry trusses can be used in space crane manipulator applications to aid in orbital construction tasks.

Comparing structural stiffness trends of idealized and realistic two-dimensional truss models gave an understanding of the causes of stiffness reduction (previous structural analyses have used only simpler idealized truss models). Two mechanisms of structural stiffness reduction were identified: reduced effective truss bending stiffness (EI) from shortening batten actuators (affecting both truss models) and batten bending in articulated geometries due to the hinge offsets in the offset-truss model.

An analytic example was also developed for comparison to finite element computed stiffness values. The stiffness values compared to within 0.1% verifying that the modeling technique used to capture batten bending was correct.

From these causes, strategies to alleviate the stiffness reduction of the truss were developed. Two types of improvement for the truss stiffness were presented. The first type contains the strategies modifying the truss but not affecting its initial straight geometry, and the second type is an alternate initially curved geometry. Strategies in the first part include distributed actuation using multiple actuators, extending the actuators, and increasing the battens' bending stiffness. Distributed actuation and increasing the battens' bending

stiffness 10 times improved the offset-truss stiffness value to near the ideal-truss stiffness throughout the range of articulation. If actuator extension is allowed, the same offset truss can operate with structural stiffness several times higher than a similar ideal truss with shortening actuators.

An adaptive truss used as an articulated arm will generally have a curved operational configuration; hence, it will seldom be in its deployed straight geometry where its stiffness is greatest. An articulating truss is a true or perfect truss structure in only one position; the deployed geometry giving the true truss structure can be chosen. The initial deployed truss geometry was modified to be curved rather than straight so that the truss begins within its operating region. The maximum stiffness value was shifted to the curved position, and the truss operates near its maximum stiffness. A circular arc was used as the basis of the curved truss to give a repeatable geometry and allow for compact packaging like the initially straight truss.

Analysis of a three-dimensional truss model demonstrated that as the initial design curvature was increased, the amount of root torsion in the first bending mode increased causing a decrease in the first mode's peak stiffness. The initially curved truss peak stiffness remained above the straight truss stiffness after articulating to that same geometry.

Appendix: Solutions to Truss Kinematics

Determine the angles in the ideal truss (Fig. 3):

$$\phi = \cos^{-1}\left[\frac{d_1^2 - 2hd_1}{2l(h-d_1)}\right] - \frac{\pi}{2} \qquad \beta = \cos^{-1}\left(\frac{l}{c} + \frac{2hd_1 - d_1^2}{2lc}\right)$$

$$\alpha = \cos^{-1}\left[\frac{h}{c} + \frac{d_2^2}{2c(h-d_2)}\right] \qquad \omega = \pi - \phi - \beta - \alpha \quad \text{(A1)}$$

$$c = (l^2 + h^2)^{\frac{1}{2}}$$

The node coordinates are then given in terms of the angles:

$$\begin{aligned} x_1 &= 0 & y_1 &= d_1 \\ x_2 &= 0 & y_2 &= h \\ x_3 &= l\cos\phi & y_3 &= y_1 - l\sin\phi \\ x_4 &= x_3 + (h-d_2)\cos\omega & y_4 &= y_3 + (h-d_2)\sin\omega \end{aligned} \quad \text{(A2)}$$

Note that the location and orientation of the first batten is known, and in this case is taken to be vertical at the origin. Each bay that follows will base its geometry on the previous bay so that an actuator will affect all of the bays that follow it in the truss.

Three length constraint equations are needed for each bay of the offset-truss:

$$\begin{aligned} (x_6 - x_3)^2 + (y_6 - y_3)^2 - l_A^2 &= 0 \\ (x_7 - x_4)^2 + (y_7 - y_4)^2 - c_A^2 &= 0 \\ (x_8 - x_5)^2 + (y_8 - y_5)^2 - l_A^2 &= 0 \end{aligned} \quad \text{(A3)}$$

The offset node coordinates of the next batten (nodes 6–10 in Fig. 4) are related to a single point on that batten (node 9 is the node point chosen):

$$\begin{aligned} x_6 &= x - l_3\cos\theta & y_6 &= y + l_3\sin\theta \\ x_7 &= x - n_x\cos\theta & y_7 &= y + n_y\cos\theta \\ x_8 &= x_{10} - l_1\cos\theta & y_8 &= y_{10} + l_1\sin\theta \\ x_{10} &= x + (h-d_2)\sin\theta & y_{10} &= y + (h-d_2)\cos\theta \end{aligned} \quad \text{(A4)}$$

By substituting Eqs. (A4) into Eqs. (A3), the vector constraint function f of three equations in three unknowns (x, y, and θ) is given to determine the position of the second batten in terms of the known values

$$f = \begin{bmatrix} (x - l_3\cos\theta - x_3)^2 + (y + l_3\sin\theta - y_3)^2 - l_A^2 \\ (x - n_x\cos\theta - x_4)^2 + (y + n_y\sin\theta - y_4)^2 - c_A^2 \\ \left[(x + (h-d_2)\sin\theta - l_1\cos\theta - x_5)^2\right. \\ \left. \quad + (y + (h-d_2)\cos\theta + l_1\sin\theta - y_5)^2 - l_A^2\right] \end{bmatrix} = \mathbf{0} \quad \text{(A5)}$$

As is seen in Eq. (A5), the three unknowns are coupled and cannot be solved for directly as was the case for the ideal truss; an iterative solution is required. Note that the ideal-truss kinematics provides an excellent initial guess.

References

[1]Mikulas, M. M., Davis, R. C., and Greene, W. H., "A Space Crane Concept: Preliminary Design and Static Analysis," NASA TM-101498, Nov. 1988.

[2]Wu, K. C., and Sutter, T. R., "Structural Analysis of Three Space Crane Articulated-Truss Joint Concepts," NASA TM-4373, May 1992.

[3]Dorsey, J. T., Sutter, T. R., and Wu, K. C., "Structurally Adaptive Space Crane Concept for Assembling Space Systems on Orbit," NASA TP-3307, Nov. 1992.

[4]Rhodes, M. D., and Mikulas, M. M., "Deployable Controllable Geometry Truss Beam," NASA TM-86366, June 1985.

[5]Mikulas, M. M., Jr., Rhodes, M. D., and Simonton, J. W., "Deployable Geodesic Truss Structure," U.S. Patent 4677803, July 1987.

[6]Stewart, D., "A Platform with Six Degrees of Freedom," *Proceedings of the Institute of Mechanical Engineers*, Mechanical Engineering Publications for the Inst. of Mechanical Engineers, London, Vol. 180, Pt. 1, 1965–66, pp. 371–386.

[7]Miura, K., and Furuya, H., "Variable Geometry Truss and Its Application to Deployable Truss and Space Crane Arm," *Acta Astronautica*, Vol. 12, No. 7/8, 1985, pp. 599–607.

[8]Miura, K., and Furuya, H., "Adaptive Structure Concept for Future Space Applications," *AIAA Journal*, Vol. 26, No. 8, 1988, pp. 995–1002.

[9]Hughes, P. C., Sincarsin, W. G., and Carroll, K. A., "Trussarm—A Variable-Geometry-Truss Manipulator," *Journal of Intelligent Materials Systems and Structures*, Vol. 2, April 1991, pp. 148–160.

[10]Chen, G. S., and Wada, B. K., "Adaptive Truss Manipulator Space Crane Concept," *Journal of Spacecraft and Rockets*, Vol. 30, No. 1, 1993, pp. 111–115.

[11]Mabie, H. H., and Reinholtz, C. F., *Mechanisms and Dynamics of Machinery*, 4th ed., Wiley, New York, 1987, pp. 583–587.

[12]Das, S. K., Utku, S., and Wada, B. K., "Inverse Dynamics of Adaptive Structures Used as Space Cranes," *Journal of Intelligent Materials Systems and Structures*, Vol. 1, Jan. 1990, pp. 50–75.

[13]Padmanabhan, B., Arun, V., and Reinholtz, C. F., "Closed-Form Inverse Kinematic Analysis of Variable Geometry Truss Manipulators," *Journal of Mechanical Design*, Vol. 114, No. 3, 1992, pp. 438–443.

[14]Tanaka, M., Seguchi, Y., and Hanahara, K., "Kinematics of Adaptive Truss Permiting Nodal Offset (Configuration and Workspace Reach)," *Journal of Intelligent Materials Systems and Structures*, Vol. 2, July 1991, pp. 301–327.

[15]Mikulas, M. M., Jr., Wada, B. K., Farhat, C., Thorwald, G., and Withnell, P., "Initially Deformed Truss Geometry for Improving the Adaptive Performance of Truss Structures," 3rd International Conf. on Adaptive Structures (San Diego, CA), International Society for Optical Engineering, SPIE Vol. 2040, Technomic, Lancaster, PA, 1992, pp. 305–319.

[16]Thorwald, G., "A Structural Design Methodology for Large Angle Beam Trusses Considering Offset Joint Modeling," Ph.D. Dissertation, Aerospace Engineering Dept., Univ. of Colorado, Boulder, CO, Aug. 1994.

[17]Blevins, R. D., *Formulas for Natural Frequency and Mode Shape*, 1st ed., Van Nostrand Reinhold, Princeton, NJ, 1979, p. 158.

[18]Hinkle, J. D., and Peterson, L. D., "Experimental Dynamic Characterization of a Reconfigurable Adaptive Precision Truss," AIAA Paper 94-1734, April 1994.

[19]Beer, F. P., and Johnston, E. R., Jr., *Mechanics of Materials*, 1st ed., McGraw–Hill, New York, 1981, p. 511.

E. A. Thornton
Associate Editor